

**Title**

4D-flow MRI Can Quantitatively Assess Portosystemic Shunt Severity and Confirm  
Normalization of Portal Flow After Embolization of Large Portosystemic Shunts

**Short running title**

4D-flow MRI for portosystemic shunts

**Authors**

Ryota Hyodo<sup>1\*</sup>, Yasuo Takehara<sup>1,2</sup>, Takashi Mizuno<sup>3</sup>, Kazushige Ichikawa<sup>3</sup>, Yoji  
Ishizu<sup>4</sup>, Masataka Sugiyama<sup>1,2</sup>, Shinji Naganawa<sup>1</sup>

**Authors' affiliations**

<sup>1</sup> Department of Radiology, Nagoya University Graduate School of Medicine, 65  
Tsurumai-cho, Showa-ku, Nagoya 466-8550, Japan

<sup>2</sup> Department of Fundamental Development for Advanced Low Invasive Diagnostic  
Imaging, Nagoya University Graduate School of Medicine, 65 Tsurumai-cho, Showa-  
ku, Nagoya 466-8550, Japan

<sup>3</sup> Department of ~~Medical~~Radiological Technology, Nagoya University Hospital, 65

Tsurumai-cho, Showa-ku, Nagoya 466-8550, Japan

<sup>4</sup> Department of Gastroenterology and Hepatology, Nagoya University Graduate  
School of Medicine, 65 Tsurumai-cho, Showa-ku, Nagoya 466-8550, Japan

**Corresponding author:** Ryota Hyodo

Department of Radiology

Nagoya University Graduate School of Medicine

65 Tsurumai-cho, Showa-ku, Nagoya 466-8550, Japan

E-mail: [ryouta771@med.nagoya-u.ac.jp](mailto:ryouta771@med.nagoya-u.ac.jp)

Tel: +81-52-744-2327

Fax: +81-52-744-2335

**Abstract**

Diagnosis and severity assessments of portosystemic shunts (PSSs) are important because the pathology sometimes results in severe hepatic encephalopathy (HE), which can be treated almost completely by shunt embolization. At present, morphological assessment of PSS is performed mainly by computed tomography, and ultrasound is used for blood flow assessment. In two cases of PSS-related HE, we used time-resolved 3D cine phase-contrast (4D-flow) magnetic resonance imaging (MRI) to assess blood flow before and after shunt embolization. Before the intervention, blood flow in the main trunk of the superior mesenteric vein (SMV) was mostly hepatofugal. However, post-interventional 4D-flow MRI revealed hepatopetal SMV flow with significantly increased portal vein blood flow. 4D-flow MRI is an ideal adjunct to Doppler ultrasonography, allowing for objective and visual assessment of morphology and blood flow of the portal venous system, including PSSs, and is useful in determining the indications for, and outcome of, PSS embolization.

**Key words**

4D-flow MRI, hepatic encephalopathy, portal hemodynamics, portosystemic shunts,

shunt embolization

## **Introduction**

Hepatic encephalopathy (HE) is one of the most debilitating manifestations of liver disease and has a poor prognosis.<sup>1</sup> Its diagnosis is based on clinical features such as neuropsychiatric disorders and asterixis, along with objective abnormalities such as elevated serum ammonia concentration and the formation of a large portosystemic shunt (PSS) on dynamic contrast-enhanced computed tomography (DCE-CT).<sup>1</sup> In addition to medical therapies such as a non-absorbable disaccharide, shunt embolization has been reported as useful in the treatment of PSS-related HE.<sup>2-</sup>

<sup>4</sup> Although PSS is diagnosed mainly by CT, Doppler ultrasound (US) is the first choice for portal blood flow evaluation, as it can easily determine the flow velocity and direction in the portal vein (PV) and portions of the superior mesenteric vein (SMV), splenic vein (SV), and collateral veins with abdominal wall proximity. However, ultrasound has some limitations, such as operator dependence and limited visualization as well as limited field of view of deep structures.

Recently, time-resolved 3D cine phase-contrast (4D-flow) magnetic resonance imaging (MRI) has facilitated the cardiac phase-resolved iso-voxel acquisition of 3D blood flow velocity information within a 3D anatomical volume throughout the cardiac cycle.<sup>5</sup> This technique also allows for simultaneous

measurements of 3D flow velocity vectors in the PV system, including the SMV, SV, and collateral circulations.<sup>5-8</sup> The usefulness of 4D-flow MRI in the PV area has been reported, and the procedural indications and therapeutic effects of portal intervention have been evaluated.<sup>9-11</sup> To our knowledge, there have been no reports describing the usefulness of 4D-flow MRI for the evaluation of portal hemodynamic patterns in PSS-related HE before and after PSS embolization. Here, we present our evaluation and management of two such cases.

## **Methods**

The internal review board approved this 4D-flow MRI study, and written informed consent for the study and the intervention was obtained from the patients and their families. This study also conforms to the provisions of the Declaration of Helsinki. Before and after the intervention, after more than 6 h of fasting, a 4D-flow MRI was conducted using a 3T MRI scanner (Prisma; Siemens AG Healthineers, Erlangen, Germany) with two 18-ch phased array coils. Following coronal balanced steady-state free precession-imaging, a 3D coronal dynamic contrast-enhanced MRI was obtained for morphological imaging, using 0.1 mmol/kg of gadobutrol (Gadovist; Bayer Yakuhin, Osaka, Japan) with an injection rate of 1 mL/s.

Subsequently, retrospective electrocardiogram-gated 4D-flow MRI with respiratory navigator-gate was conducted, including the entire abdomen, with the parameters listed in Table 1.

The 4D-flow data set, segmented by morphological imaging, was post-processed using flow analysis software (iTFlow; Cardio Flow Design, Tokyo, Japan). The main PV, SMV, SV, and main collateral veins were visualized by 3D vector field and streamlines. The flowmetries were performed by placing a region of interest on the cross-sections of these vessels, avoiding non-laminar flow portions.

## **Results**

### **Case 1**

A 75-year-old woman with tremors was referred to our hospital. The patient had liver dysfunction (Table 2, Model for End-Stage Liver Disease [MELD] score 7), elevated serum ammonia concentration (205 mg/dL), and asterixis, which resulted in a diagnosis of Grade II HE. DCE-CT showed a mild liver deformity and a large meso-caval shunt (2 inflows from the SMV and 5 outflows to the inferior vena cava [IVC]). A liver biopsy revealed non-alcoholic steatohepatitis (NASH) and

liver fibrosis of degree F2.<sup>12</sup> Medical treatment for HE (lactulose and rifaximin) was initiated; however, the effect was insufficient and the symptoms of HE persisted. Liver function was relatively maintained; therefore, PSS was considered to be the main cause of HE. 4D-flow MRI was performed to evaluate the portal hemodynamic patterns before shunt embolization.

4D-flow MRI (Fig 1a) showed peripheral dilation of the SMV and shunting to the IVC. Blood flow in the SMV trunk and branches was retrograde at 3.7 mL/s in the SMV trunk. The main PV received blood flow from the SV at 4.4 mL/s, which is lower than normal. These findings confirmed that almost all intestinal blood flow was to the systemic circulation, which was the main cause of HE. Doppler US also showed decreased portal blood flow and SMV trunk regurgitation, but the deep shunt area was difficult to evaluate. The maximum flow velocity (Vmax) in the main PV was 13.5 cm/s on 4D-flow MRI and 14.7 cm/s on US, confirming similar results. Using the percutaneous transhepatic method, digital subtraction angiography (DSA) of the SMV revealed flow to the IVC via the collateral vein (Fig 1b). Following coil embolization of the two main feeders of the meso-caval shunt, DSA of the SMV showed that blood flow had become antegrade, and the PV branches had opacified (Fig 1c).

Post-interventional 4D-flow MRI (Fig 1d) was performed on the same day, revealing that collateral blood flow could hardly be identified, and blood flow in the SMV trunk and branches had become antegrade. The main PV blood flow increased to 14.6 mL/s, probably associated with an unexplained increase in SV blood flow. Concurrently performed US also showed antegrade SMV and increased main PV blood flow. The Vmax of the main PV was 26.5 cm/s on 4D-flow MRI and 24.3 cm/s on US. Immediately after the intervention, the symptoms of HE disappeared and the serum ammonia concentration normalized (61 mg/dL, Table 2). No recurrence of HE was observed for four months without medication.

## Case 2

A 57-year-old woman with impaired consciousness and hyperammonemia was referred to our hospital. With mild liver dysfunction (Table 2, MELD score 8), elevated serum ammonia concentration (107 mg/dL), and a fatty, mildly deformed liver on CT, she was diagnosed with HE. A large SMV-right internal iliac vein (RIIV) shunt was also observed on DCE-CT. A liver biopsy revealed NASH and liver fibrosis of degree F2.<sup>12</sup> Initially, medical treatment (lactulose and BCAA supplementation) was administered; however, the effect was insufficient and the

symptoms of HE persisted. Therefore, this case was also considered to be PSS-related HE, and 4D-flow MRI was performed to evaluate the hemodynamic patterns of the portal circulation and collaterals.

4D flow MRI (Fig 2a) showed substantial collateral circulation from the SMV to the RIIV via the inferior mesenteric vein (IMV), with a hepatofugal flow of 6.9 mL/s. The main PV was narrowed, with the average flow volume decreased to approximately 1.5 mL/s. Blood flow in the SMV trunk, which is located cephalad to the IMV junction, was retrograde. Therefore, most blood from the intestines did not flow into the main PV but into the collateral vein, indicating that the SMV-RIIV shunt was the main cause of HE. This patient had no available flow velocity measurements performed using US. During the interventional procedure, a 5-French guiding sheath (Destination; Terumo, Tokyo, Japan) was placed in the shunt vessel via the RIIV by approaching from the left common femoral vein. Subsequently, the SMV was selected with a 4-French catheter (Hanaco Medical, Saitama, Japan). DSA from the SMV (Fig 2b) showed that although there was a slight flow to the main PV, most flow was to the collaterals, supporting the findings of the pre-interventional 4D-flow MRI. **Following coil embolization from the collateral vein to the orifice of the IMV, DSA of the collateral vein (Fig 2c) showed that the orifice**

of the IMV was well embolized and the portal system was not visualized.

Post-interventional 4D-flow MRI (Fig 2ed) performed the next day showed that the visualization of the main PV to the intrahepatic branches was improved, and the blood flow in the main PV also increased to 4.8 mL/s. In addition, SMV trunk blood flow became antegrade, indicating that intestinal blood flow had become hepatopetal into the PV. The serum ammonia concentration immediately normalized (62 mg/dL, Table 2), and the symptoms of HE improved. Although BCAAs were discontinued, serum ammonia concentrations remained normal and no recurrence of HE was observed for seven months.

## **Discussion**

Development of extensive hepatofugal collateral circulation is one of the causes of HE.<sup>1-4</sup> The diagnosis of PSS-related HE is important because embolization of the PSS can improve symptoms.<sup>2-4</sup> In the present two cases, 4D-flow MRI allowed for a comprehensive evaluation of portal hemodynamic patterns, facilitating a visual and objective grasp of the pathophysiology of the disease and assessment of therapeutic effect. In both cases, pre-interventional 4D-flow MRI confirmed retrograde flow in the SMV trunk, with most blood from the intestinal

tract flowing into the systemic circulation; this was thought to be the main cause of HE. Post-interventional 4D-flow MRI confirmed a marked decrease or disappearance of collateral circulation, antegrade SMV flow, and increased main PV blood flow. The fact that 4D-flow MRI was able to objectively predict improvement in HE immediately after treatment shows its utility for early evaluation of the treatment effect.

Doppler US is the first choice for assessing portal blood flow because it can easily evaluate the direction and velocity of flow.<sup>13, 14</sup> In case 1, the decrease in PV blood flow and SMV trunk regurgitation could be assessed adequately by US. However, US has some limitations, such as relatively low intra- and inter-observer agreement, relatively poor reproducibility, limited field of view, limited visualization of complex structures, and image quality hampered by obesity or gastrointestinal gas.<sup>7-9, 13, 14, 15, 16</sup> In contrast, 4D-flow MRI is characterized by comprehensive data sampling of complete velocity and morphology, followed by objective retrospective data analysis.<sup>6-11</sup> No special expertise is needed in collecting and analyzing the data of 4D-flow. The acquired data can be displayed in a 3D cine fashion, thereby facilitating the understanding of the pathology and treatment effects. In case 2, we could not compare US and 4D-flow MRI because we did not

evaluate portal vein velocity by US before and after treatment. However, 4D-flow MRI has full spatial and temporal data; therefore, retrospective flowmetries are feasible even after a patient has left the MR suite. The low cost and the ability to perform repeated bedside examinations are advantages of US.<sup>13, 17</sup> 4D-flow MRI may be a powerful adjunct to US in determining the therapeutic indications and post-treatment evaluation of PSS-related HE. On the other hand, DCE-CT can assess the location and detailed morphology of the PSS in a shorter period of time than MRI; however, it does not reveal the rate or direction of flow. In fact, there are some cases in which the formation of a large PSS does not cause clinically problematic HE.<sup>18</sup> In these cases, it is possible that there is predominantly SV flow or a non-problematic amount of SMV flow into the systemic circulation; these possibilities can be evaluated by 4D-flow MRI. **Angiography can evaluate the direction of SMV blood flow and the opacity of portal vein before and after intervention; however, post-interventional evaluation is difficult when the intervention is performed from the femoral vein in a retrograde fashion, as in case 2. In addition, angiography is not an intrinsically physiological procedure. The insertion of the sheath or catheter itself may alter the physiological portal venous flow. Compared to angiography, 4D-flow MRI can evaluate portal hemodynamics**

in a physiological state.

To evaluate the validity of the 4D-flow MRI measurements, we performed a preliminary phantom experiment using the same MRI system. PV blood flow was assumed to be at steady state, and flow was evaluated simultaneously with an ultrasonic flowmeter (Keyence Corp., Osaka, Japan) (time resolution, 3.3 ms) and 4D-flow MRI (time resolution, 50 ms; velocity encoding 100 cm/s). The average flows were 10.6 mL/s and 10.5 mL/s for the ultrasonic flowmeter and 4D flow MRI, respectively, and the relative error was -0.19 %, which was not significantly different (unpublished data). These results validate the accuracy of the flowmetry of 4D-flow MRI in this study.

4D-flow MRI has several limitations. First, it requires relatively lengthy imaging time. Concerning the present two cases, the 4D-flow MRI alone took 10 minutes and 17 minutes for imaging, respectively. In addition, the time required for positioning and morphological images for segmentation. In the Cartesian technique that we are currently using, the imaging time for the portal system usually requires 10-15 minutes. Patients with hepatic encephalopathy may not be able to lie still on the examination bed despite the technicians' instruction. However, methods to shorten the imaging time have been developed, and it has been reported that the

imaging time can be significantly shortened to a few minutes or even less by employing the compressed sensing<sup>19</sup> or the spiral method<sup>20</sup>. The widespread use of these innovations will further reduce the imaging time to breath-holding level. Second, present spatial resolution of 1.4 mm or 1.5 mm may not be sufficient to evaluate small intrahepatic portal branches and small collateral vessels; however, the limitation will be improved in the future with combined use of artificial intelligence<sup>21</sup>.

In conclusion, we have reported the first use of 4D-flow MRI for hemodynamic evaluations in two patients with PSS-related HE before and after an interventional procedure. 4D-flow MRI is feasible and may complement US in planning therapeutic indications and assessing therapeutic effects for patients with PSS-related HE.

### **Acknowledgments**

The authors thank Y. Kato, R.T. and Y. Sakurai, R. T. for their technological assistance in image acquisitions, and Komori Y., Siemens Healthcare for providing the pre-product version of the 4D-flow MR application.

### **Declaration of Conflict of Interest**

The second author Yasuo Takehara is an endowed chair of Nagoya University supported by a private company Himedic Nagoya and the sixth author Masataka Sugiyama is similarly an endowed assistant professor; however, the status is irrelevant to the contents of this paper. Other authors have no conflicts of interest to disclose. This work was supported by JSPS KAKENHI Grant Number JP19K17165.

### **References**

1. Vilstrup H, Amodio P, Bajaj J, et al. Hepatic encephalopathy in chronic liver disease: 2014 Practice Guideline by the American Association for the Study of Liver Diseases and the European Association for the Study of the Liver. *Hepatology* 2014; 60: 715-35.
2. Laleman W, Simon-Talero M, Maleux G, et al. Embolization of large spontaneous portosystemic shunts for refractory hepatic encephalopathy: a multicenter survey on safety and efficacy. *Hepatology* 2013; 57: 2448-57.
3. Naeshiro N, Kakizawa H, Aikata H, et al. Percutaneous transvenous embolization for portosystemic shunts associated with encephalopathy: Long-term outcomes in 14

patients. *Hepatol Res* 2014; 44: 740-9.

4. Lynn AM, Singh S, Congly SE, et al. Embolization of portosystemic shunts for treatment of medically refractory hepatic encephalopathy. *Liver Transpl* 2016; 22: 723-31.

5. Markl M, Chan FP, Alley MT, et al. Time-resolved three-dimensional phase-contrast MRI. *J Magn Reson Imaging* 2003; 17: 499-506.

6. Frydrychowicz A, Landgraf BR, Nieszpodzany E, et al. Four-dimensional velocity mapping of the hepatic and splanchnic vasculature with radial sampling at 3 tesla: a feasibility study in portal hypertension. *J Magn Reson Imaging* 2011; 34: 577-84.

7. Motosugi U, Roldan-Alzate A, Bannas P, et al. Four-dimensional Flow MRI as a Marker for Risk Stratification of Gastroesophageal Varices in Patients with Liver Cirrhosis. *Radiology* 2019; 290: 101-7.

8. Roldan-Alzate A, Frydrychowicz A, Nieszpodzany E, et al. In vivo validation of 4D flow MRI for assessing the hemodynamics of portal hypertension. *J Magn Reson Imaging* 2013; 37: 1100-8.

9. Owen JW, Saad NE, Foster G, Fowler KJ. The Feasibility of Using Volumetric Phase-Contrast MR Imaging (4D Flow) to Assess for Transjugular Intrahepatic Portosystemic Shunt Dysfunction. *J Vasc Interv Radiol* 2018; 29: 1717-24.

10. Bannas P, Roldán-Alzate A, Johnson KM, et al. Longitudinal Monitoring of Hepatic Blood Flow before and after TIPS by Using 4D-Flow MR Imaging. *Radiology* 2016; 281: 574-82.
11. Hyodo R, Takehara Y, Mizuno T, Ichikawa K, Ogura Y, Naganawa S. Portal Vein Stenosis Following Liver Transplantation Hemodynamically Assessed with 4D-flow MRI before and after Portal Vein Stenting. *Magn Reson Med Sci* 2020. doi: 10.2463/mrms.ici.2020-0057. Online ahead of print.
12. Kleiner DE, Brunt EM, Van Natta M, et al. Design and validation of a histological scoring system for nonalcoholic fatty liver disease. *Hepatology* 2005; 41: 1313-21.
13. Abdelaziz O, Attia H. Doppler ultrasonography in living donor liver transplantation recipients: Intra- and post-operative vascular complications. *World J Gastroenterol* 2016; 22: 6145-72.
14. Görg C, Riera-Knorrenschild J, Dietrich J. Pictorial review: Colour Doppler ultrasound flow patterns in the portal venous system. *Br J Radiol* 2002; 75: 919-29.
15. Maruyama H, Kato N. Advances in ultrasound diagnosis in chronic liver diseases. *Clin Mol Hepatol* 2019; 25: 160-7.
16. Lee SS, Park SH. Radiologic evaluation of nonalcoholic fatty liver disease. *World J Gastroenterol* 2014; 20: 7392-402.

17. Procopet B, Berzigotti A. Diagnosis of cirrhosis and portal hypertension: imaging, non-invasive markers of fibrosis and liver biopsy. *Gastroenterol Rep (Oxf)* 2017; 5: 79-89.
18. Qi X, Qi X, Zhang Y, et al. Prevalence and Clinical Characteristics of Spontaneous Splenorenal Shunt in Liver Cirrhosis: A Retrospective Observational Study Based on Contrast-Enhanced Computed Tomography (CT) and Magnetic Resonance Imaging (MRI) Scans. *Med Sci Monit.* 2017; 23: 2527-34.
19. Neuhaus E, Weiss K, Bastkowski R, Koopmann J, Maintz D, Giese D. Accelerated aortic 4D flow cardiovascular magnetic resonance using compressed sensing: applicability, validation and clinical integration. *J Cardiovasc Magn Reson* 2019; 21: 65.
20. Dyvorne H, Knight-Greenfield A, Jajamovich G, et al. Abdominal 4D flow MR imaging in a breath hold: combination of spiral sampling and dynamic compressed sensing for highly accelerated acquisition. *Radiology* 2015; 275: 245-54.
21. Retson TA, Besser AH, Sall S, Golden D, Hsiao A. Machine Learning and Deep Neural Networks in Thoracic and Cardiovascular Imaging. *J Thorac Imaging* 2019; 34:192-201.

### Figure legends

Figure 1. A 75-year-old female with hepatic encephalopathy (Case 1). (a) Whole streamline image and expanded vector image around the superior mesenteric vein (SMV) trunk (curved arrow) by 4D-flow MRI before the intervention. Blood flow in the SMV trunk was retrograde and collateral veins (CV; circle) to the inferior vena cava had formed in the periphery of the SMV. Blood flow in the main portal vein (PV) was derived from the splenic vein. (b) Digital subtraction angiography (DSA) of the SMV revealed retrograde blood flow in the SMV trunk. (c) DSA of the SMV after shunt embolization showed that blood flow in the SMV was antegrade and the portal branches had opacified. (d) Whole streamline image and expanded vector image around the SMV (curved arrow) by 4D-flow MRI after coil embolization. The SMV blood flow had become antegrade, the blood flow in the CV (circle) was significantly reduced, and blood flow in the main PV was elevated. IVC, inferior vena cava.

Figure 2. A 57-year-old female with hepatic encephalopathy (Case 2). (a) Whole streamline image and expanded vector image around the superior mesenteric vein (SMV) trunk (curved arrow) by 4D-flow MRI before the intervention. Blood flow

in the SMV trunk was retrograde and mostly flowed through the dilated collateral vein (CV). Most flow in the main portal vein (PV) was derived from the splenic vein. (b) Digital subtraction angiography (DSA) of the SMV revealed that most blood from the SMV flowed to the CV. (c) DSA of the CV revealed that the orifice of collateral vein was well embolized and the portal system was not visualized. (d) Whole streamline image and expanded vector image around the SMV (curved arrow) by 4D-flow MRI after shunt embolization. Blood flow in the SMV was antegrade, and flow in the main PV was increased.

**Table 1.** 4D-flow MRI parameters

---

slab orientation	coronal
TR (ms)	17-18
TE (ms)	2.7-3.2
flip angle (°)	8
number of excitations	1
temporal resolution (ms)	66-72
field of view (mm)	400-440 × 400-440
voxel size (mm <sup>3</sup> )	1.4-1.5 × 1.4-1.5 × 1.4- 1.5
velocity encoding (cm/s)	50-80
parallel imaging factor	3
acquisition time (min)	10-17
time frames per R-R intervals	15

---

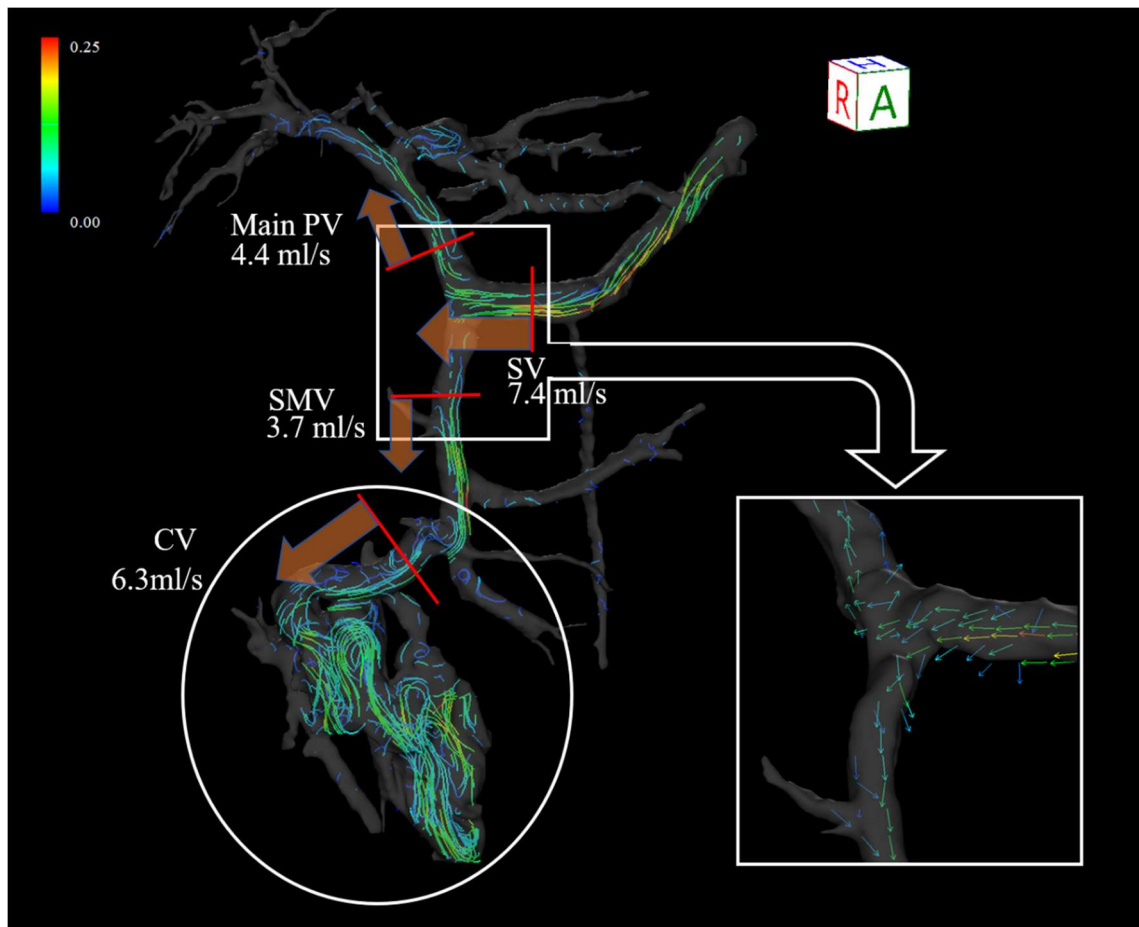
**Table 2.** Pre- and post-treatment blood test results

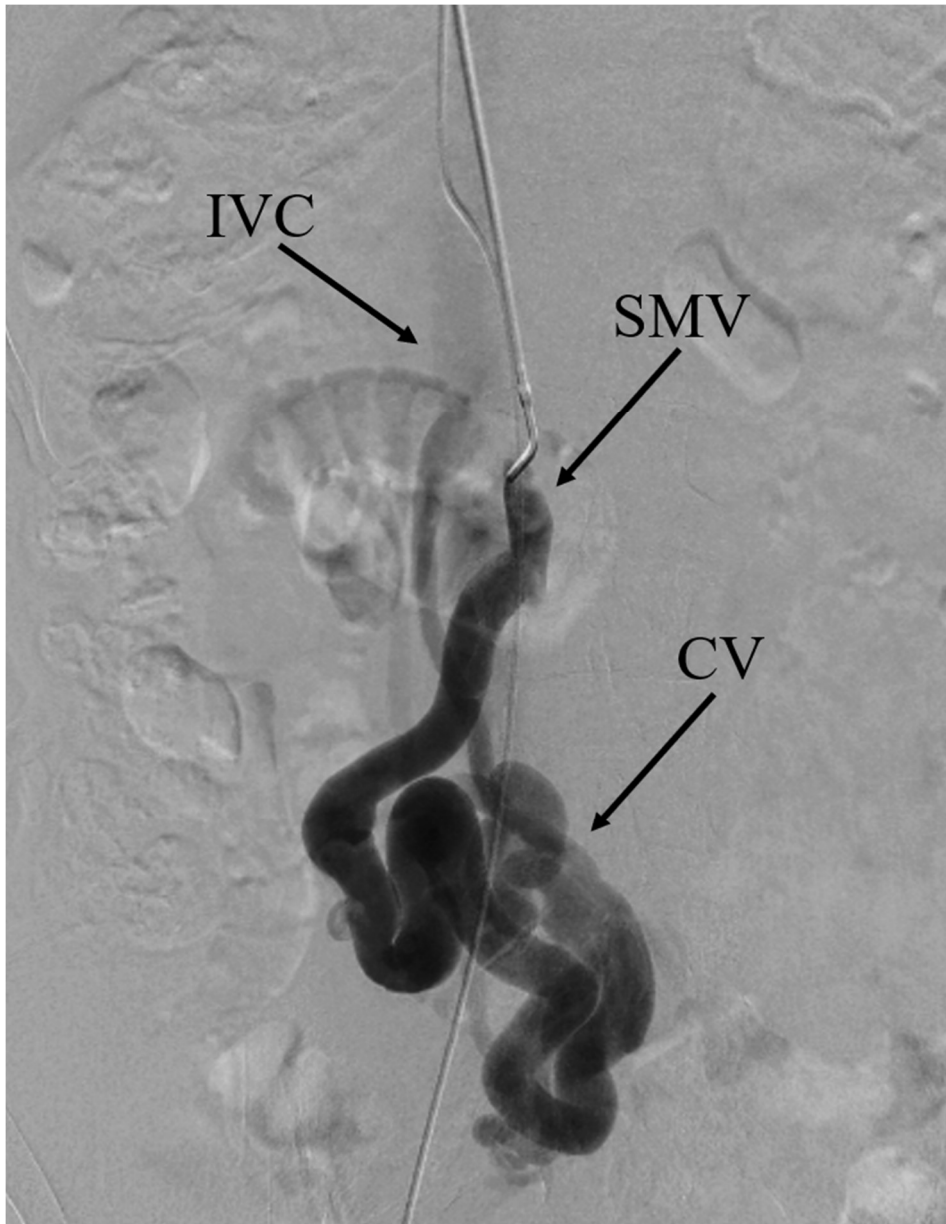
	Case 1		Case 2	
	before	1 day after	before	1 day after
T-bil	1.0	1.2	0.8	1.4
(mg/dL)				
Alb (g/dL)	4.0	3.4	3.6	3.3
PT-INR	1.05	1.10	1.14	1.21
Cre	0.69	0.68	0.40	0.39
(mg/dL)				
AST (U/L)	34	36	56	55
ALT (U/L)	26	30	38	36
Plt	195	137	133	108
( $\times 10^3/\mu\text{L}$ )				
NH <sub>3</sub>	205	61	107	62
( $\mu\text{g/dL}$ )				
MELD	7	8	8	10
score				

T-bil, total bilirubin; Alb, albumin; PT-INR, prothrombin time-international

normalized ratio; Cre, creatinine; AST, aspartate aminotransferase; ALT, alanine aminotransferase; Plt, platelets; NH<sub>3</sub>, serum ammonia concentration; MELD, Model for End-Stage Liver Disease

Figure 1a



**Figure 1b**

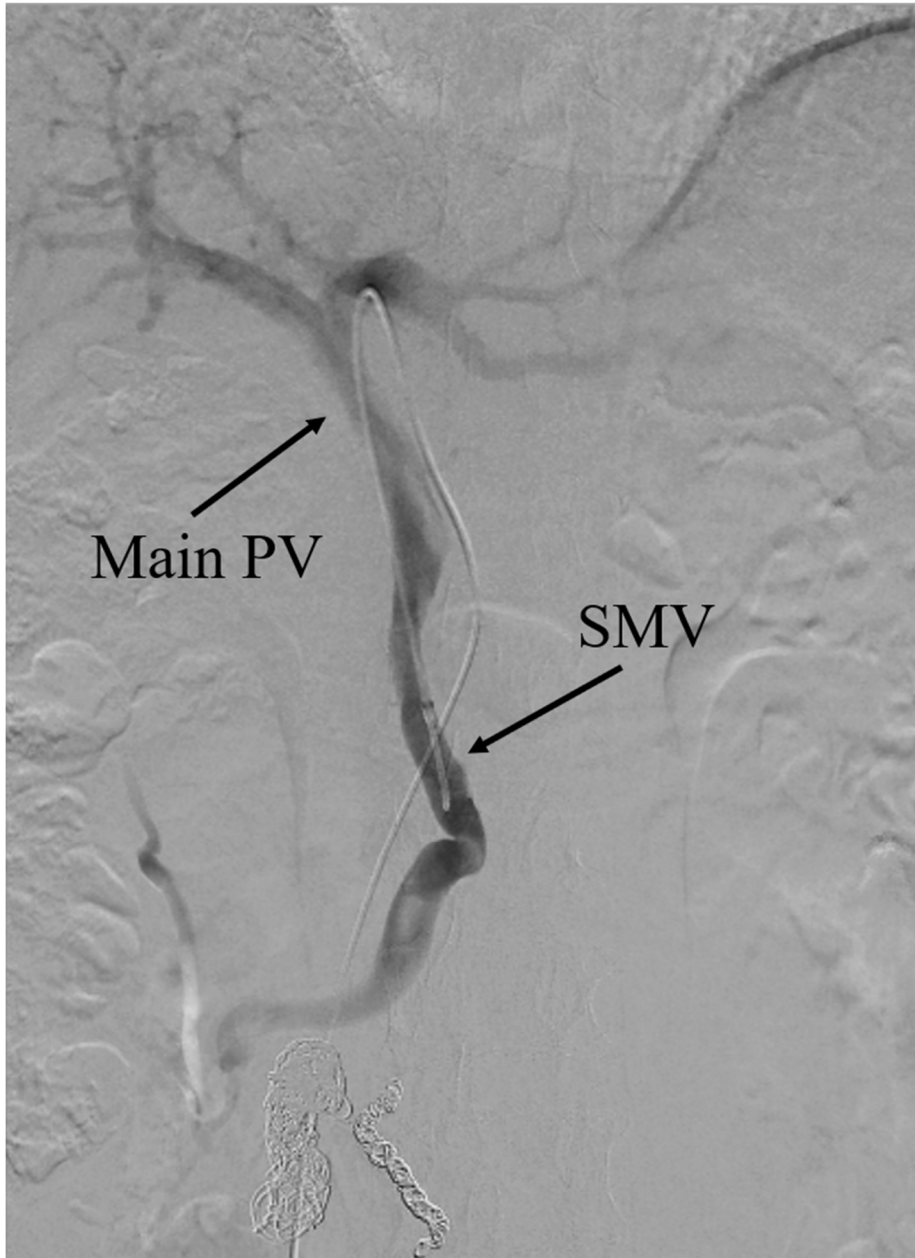
**Figure 1c**

Figure 1d

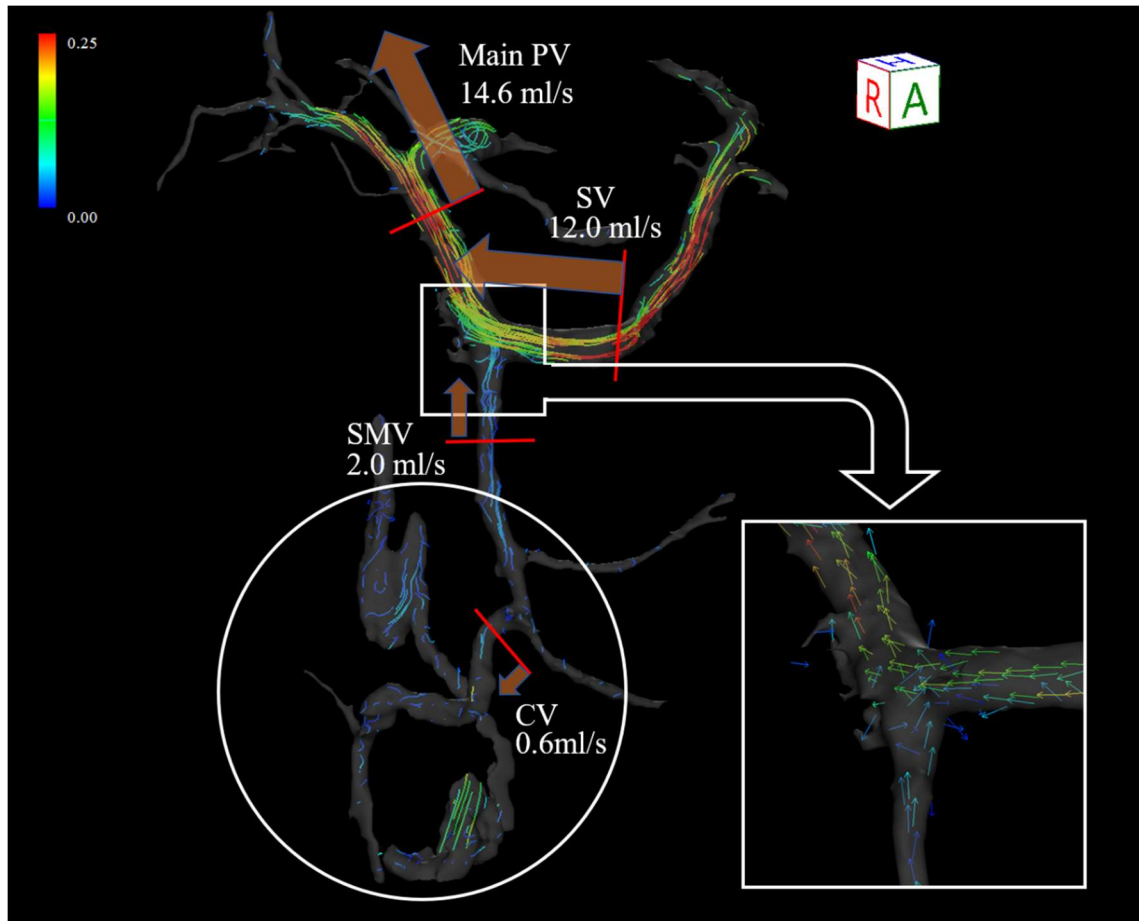


Figure 2a

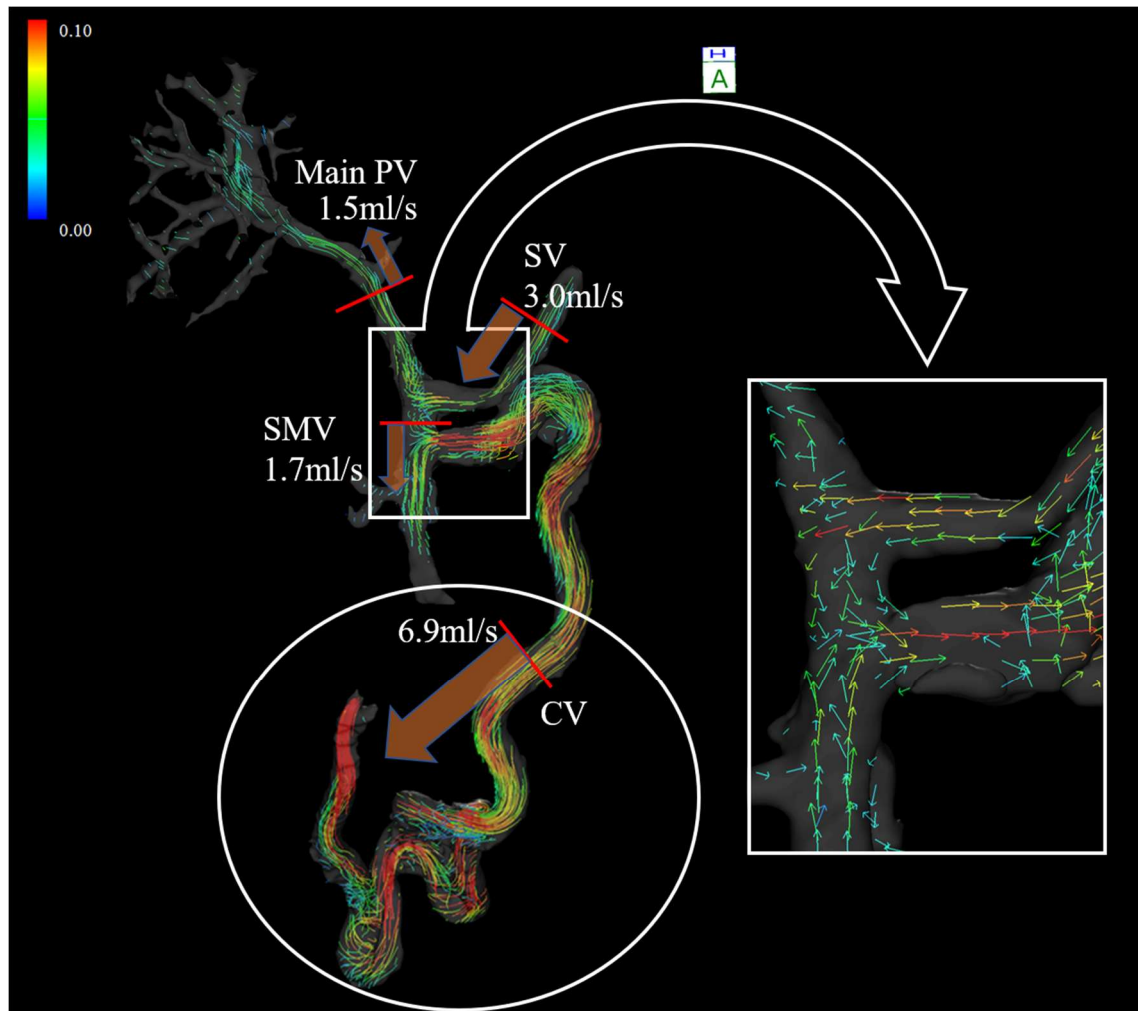
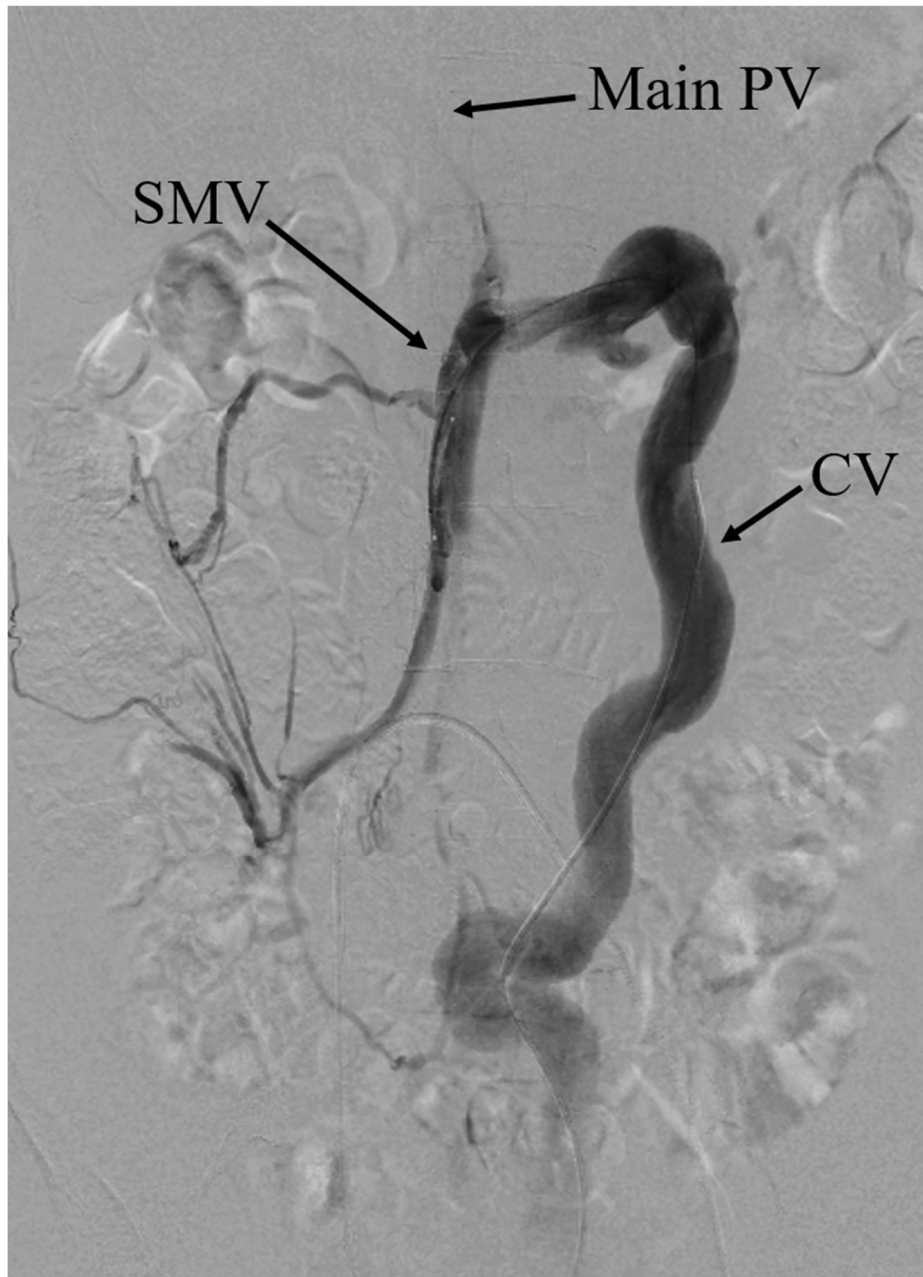


Figure 2b



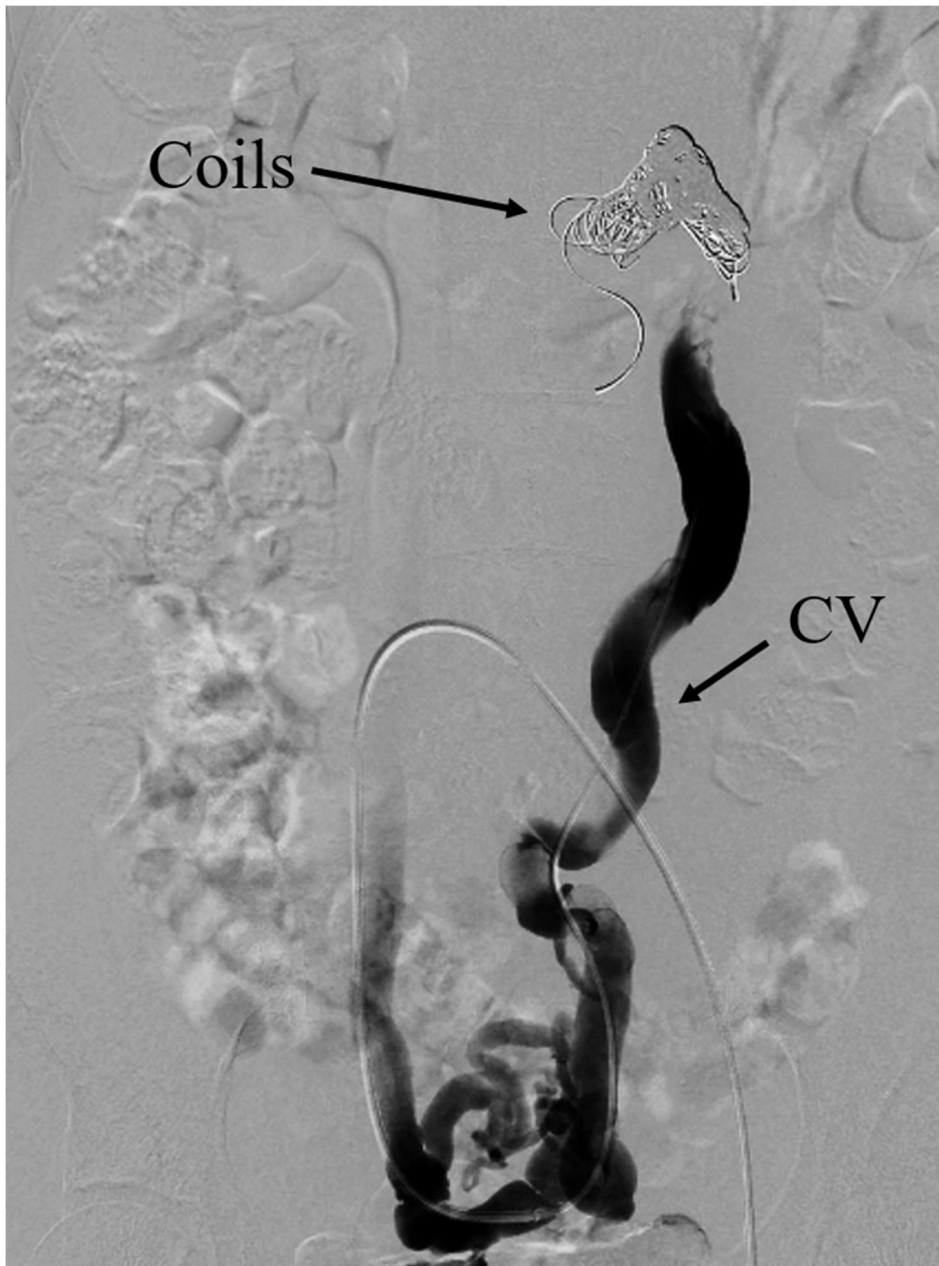
**Figure 2c**

Figure 2d

